Original article

Folia Neuropathologica

Spatial patterns of β-amyloid (Aβ) deposits in familial and sporadic Alzheimer's disease

Richard A. Armstrong

Vision Sciences, Aston University, Birmingham B4 7ET, UK

Folia Neuropathol 2011; 49 (3): 153-161

Abstract

The spatial patterns of the diffuse, primitive, and classic β-amyloid (Aβ) deposits were compared in cortical regions in early-onset familial Alzheimer's disease (EO-FAD) linked to mutations of the amyloid precursor protein APP) or presenilin 1 (PSEN1) genes, late-onset familial AD (LO-FAD), and sporadic AD (SAD). The objective was to determine whether genetic factors influenced the spatial patterns of the Aβ deposits. Aβ deposits were distributed either in clusters which were regularly distributed parallel to the pia mater or in larger, non-regularly distributed clusters. There were no significant differences in spatial pattern of the diffuse deposits between patient groups but mean cluster size of the diffuse deposits was larger in FAD compared with SAD. Primitive Aβ deposits were more frequently distributed in regular clusters and less frequently distributed in large clusters in FAD compared with SAD. Classic Aβ deposits were more frequently distributed in regularly spaced clusters and less frequently distributed in large clusters in LO-FAD compared with EO-FAD. There were no significant differences in the spatial patterns or cluster sizes of Aβ deposits in cases classified according to apolipoprotein E (APOE) genotype. These results suggest (1) greater deposition of Aβ in the form of clusters of diffuse deposits in FAD, (2) a greater proportion of diffuse deposits may be converted to primitive deposits in SAD, (3) classic deposits are more widely distributed in EO-FAD, and (4) the presence of APOE allele ε4 has little effect on the spatial patterns of Aβ deposits.

Key words: *Alzheimer's disease (AD), spatial pattern, amyloid precursor protein (APP), presenilin 1 (PSEN1), apolipoprotein E (APOE), β-amyloid (Aβ) deposits.*

Introduction

The neuropathology of Alzheimer's disease (AD) is characterised by the formation of extracellular senile plaques (SP) and intracellular neurofibrillary tangles (NFT) [8]. The most important molecular constituent of the SP is β-amyloid (Aβ) [27], a peptide of 36-43 amino acids arising by constitutive cleavage of a trans-membrane glycoprotein amyloid precursor protein (*APP*). A variety of Aβ peptides are formed as a result of secretase cleavage of *APP* [31]. The most common of these peptides is $A\beta_{42}$, cleaved in the trans-Golgi network and found largely in discrete Aβ deposits, whereas the more soluble $A\beta_{40}$, cleaved in

Communicating author:

Dr. Richard A. Armstrong, Vision Sciences, Aston University, Birmingham B4 7ET, UK, phone 0121-359-3611, fax 0121-333-4220, e-mail: R.A.Armstrong@aston.ac.uk

the endoplasmic reticulum, is also found in association with blood vessels [41,45] and may develop later in the disease [23]. Oligomers that form on the amyloid pathways may be cytotoxic species rather than $A\beta_{42}$ [37]. The discovery of β-amyloid (Aβ) led to the formulation of the 'amyloid cascade hypothesis' (ACH), the most important model of the molecular pathology of AD developed over the last 20 years [32]. Essentially, the ACH proposes that the deposition of Aβ is the initial pathological event in AD leading to the formation of NFT, cell death, and ultimately dementia.

At least four genetic loci have been implicated in AD, viz., the *APP* gene on chromosome 21 [20,28], the *presenilin* (*PSEN*) genes on chromosomes 14 (*PSEN1*) [48] and 1 (*PSEN2*) [38], and the *apolipoprotein E* (*APOE*) gene on chromosome 19 [47]. Mutations in *APP* and *PSEN* genes may alter APP metabolism, resulting in increased deposition of Aβ, while allelic polymorphism of *APOE*, and especially the expression of the ε4 allele, may increase the proportion of the more fibrillogenic $A\beta_{42}$ formed in the tissue [18,19,25]. These genetic factors, however, may not explain the majority of AD cases [30]. Hence, early-onset AD linked to *APP* and *PSEN* mutations may account for less than 5% of the total number of cases [34]. Additional susceptibility genes and environmental factors are therefore likely to be involved in AD, especially in sporadic cases. In isolated Amish communities, for example, 24 markers have been linked to dementia [40], and several other linkage studies have shown the presence of possible AD-related genes on chromosomes 9, 10, and 12 [49].

Three morphological subtypes of Aβ deposit are observed in histological preparations of AD brain [5,22]: (1) diffuse ('pre-amyloid') deposits, in which the Aβ peptide is not aggregated into amyloid and dystrophic neuritis (DN) and paired helical filaments (PHF) are infrequent or absent, (2) primitive ('neuritic') deposits, in which the Aβ is aggregated into amyloid and is associated with DN and PHF, and (3) classic ('cored') deposits, in which Aβ is highly aggregated to form a central amyloid 'core' surrounded by a 'ring' of DN. Diffuse Aβ deposits are often spatially correlated with neuronal perikarya [1,6] and may represent the earliest stages of Aβ deposition in AD [5]. Different Aβ deposit subtypes could represent stages in the maturation of a single deposit type [5]. Hence, diffuse deposits may evolve into more mature deposits as the disease progresses [5].

Aβ deposits are often clustered in the cerebral cortex, the clusters being distributed in a regular pattern parallel to the pia mater [13,15,17], and may be the result of Aβ pathology developing in relation to the cortico-cortical and cortico-hippocampal pathways [24,44]. Hence, either toxic Aβ oligomers cause degeneration of specific cortico-cortical pathways or degeneration of cortico-cortical pathways results in the deposition of Aβ [13]. The objective of this study was to determine whether the spatial pattern of Aβ deposits in the cortex was influenced by genetic factors. Hence, the spatial patterns of diffuse, primitive, and classic Aβ deposits were studied in three groups of AD cases: (1) early-onset familial AD (EO-FAD) linked to mutations of *APP* or *PSEN1*, (2) late-onset FAD (LO-FAD) not linked to *APP* or *PSEN* genes, and (3) cases of SAD. In addition, the influence of *APOE* genotype on the spatial patterns of Aβ deposits was studied.

Material and methods

Cases

Eighteen cases of AD (details in Table I), obtained from the Brain Bank, Department of Neuropathology, Institute of Psychiatry, King's College, London, UK, were studied. Informed consent was given for the removal of all brain tissue according to the 1996 Declaration of Helsinki (as modified Edinburgh, 2000). Patients were clinically assessed and all fulfilled the 'National Institute of Neurological and Communicative Disorders and Stroke and the Alzheimer Disease and Related Disorders Association' (NINCDS/ADRDA) criteria for probable AD [52]. The histological diagnosis of AD was established by the presence of widespread neocortical SP consistent with the 'Consortium to Establish a Registry of Alzheimer Disease' (CERAD) criteria [42] and 'National Institute on Aging (NIA)-Reagan Institute' criteria [36,43]. The cases were divided into three groups: (1) EO-FAD (onset $\leq$ 65 yrs) (N = 4); two cases linked to the APP_{717} mutation and two to *PSEN1* mutations (G209V and E280A), (2) LO-FAD ($\geq$ 65 yrs) (N = 5) not associated with mutations of *APP* or *PSEN* genes, and (3) SAD (N = 9) with no evidence of familial involvement. The EO-FAD cases expressed *APOE* genotype ε2/3 or ε3/3, while two of the LO-FAD cases expressed *APOE* genotype ε3/4. Of the SAD cas-

Table I. Demographic and genetic data of the Alzheimer's disease (AD) cases studied

Case	Sex	Age	Onset	Group linkage	Genetic	*APOE* genotype
A	M	65	NA	EO-FAD	*APP717*	3/3
B	F	59	NA	EO-FAD	*APP717*	3/3
C	F	61	NA	EO-FAD	*PSEN1*	3/3
D	F	45	40	EO-FAD	*PSEN1*	2/3
E	F	72	66	LO-FAD	ND	2/3
F	F	86	80	LO-FAD	ND	3/4
G	F	77	72	LO-FAD	ND	3/3
H	F	79	68	LO-FAD	ND	3/4
I	F	85	76	LO-FAD	ND	3/3
J	M	80	77	SAD	–	3/3
K	F	87	82	SAD	–	3/4
L	F	64	59	SAD	–	4/4
M	F	91	83	SAD	–	3/4
N	M	73	66	SAD	–	2/3
O	F	82	75	SAD	–	ND
P	F	91	85	SAD	–	3/4
Q	F	86	83	SAD	–	3/4
R	F	90	NA	SAD	–	ND

APOE – apolipoprotein E, APP – amyloid precursor protein, EO-FAD – early-onset familial Alzheimer's disease, LO-FAD – late-onset familial Alzheimer's disease, SAD – sporadic Alzheimer's disease, PSEN1 – presenilin 1, M – male, F – female, ND – not determined, NA – data not available

es, four expressed *APOE* genotype ε3/4, one case ε4/4, and the remaining cases expressed genotype ε2/3 or ε3/3.

Tissue preparation

Blocks of the frontal and temporal cortex were taken at the level of the genu of the corpus callosum and lateral geniculate body respectively to study the superior frontal gyrus (SFG), superior temporal gyrus (STG) and the parahippocampal gyrus (PHG). Tissue was fixed in 10% phosphate-buffered formal saline and embedded in paraffin wax. 7 μm coronal sections were stained with a rabbit polyclonal antibody (Gift of Prof. B.H. Anderton, Institute of Psychiatry, King's College London) raised to the 12-28 amino acid sequence of the Aβ protein [50], and which distinguishes the major types of Aβ deposit [5]. The antibody was used at a dilution of 1 in 1200 and the sections incubated at 4°C overnight. Sections were pre-treated with 98% formic acid for 6 minutes, which enhances Aβ immunoreactivity. Aβ was visualised using the streptavidin-biotin horseradish peroxidase procedure with diaminobenzidine as the chromogen. Sections were also stained with haematoxylin. Aβ deposits were identified according to the criteria of Delaere *et al.* [22]: (1) diffuse deposits were 10-200 μm in diameter, lightly stained, irregular in shape, and with diffuse boundaries; (2) primitive deposits were 20-60 μm, well demarcated, symmetrical in shape, and strongly stained; and (3) classic deposits were 20-100 μm and had a distinct central amyloid core surrounded by a 'corona' of DN.

Morphometric methods

The spatial patterns of the Aβ deposits were studied parallel to the pia mater in the upper 1 mm of the cortex using a magnification of × 100 [13]. A strip of cortex 17 600 to 25 600 μm in length, and which included a sulcus and a gyrus, was studied using 1000 × 200 μm contiguous sample fields, the short dimension of the field being aligned with the surface of the pia mater [7]. Hence, the sample field included laminae I, II, and III. Between 64 and 128 contiguous sample fields were used to sample each gyrus. A micrometer grid with grid lines at intervals of 10 μm was used as the sample field. The number of diffuse, primitive, and classic Aβ deposits was counted in each field.

Data analysis

The data were analysed by spatial pattern analysis [2,10,13,14]. Essentially, the variance/mean (V/M) ratio of the data measures the degree of non-randomness present and determines whether Aβ deposits were distributed randomly (V/M = 1), regularly (V/M < 1), or in clusters (V/M > 1) along the strip of cortex parallel to the pia mater. The V/M ratio was calculated at increasing field sizes by adding together successively data from adjacent sample fields, e.g., 200 × 1000 μm (the original field size) and then at 400 × 1000 μm, 800 × 1000 μm, etc., up to a size limited by the length of cortex sampled. The V/M ratio was plotted against the increasing field size to reveal the spatial pattern. If the deposits were clustered, then the analysis indicated whether the clusters themselves were randomly or regularly distributed and provides an estimate of the mean dimension of the clusters in a plane parallel to the pia mater.

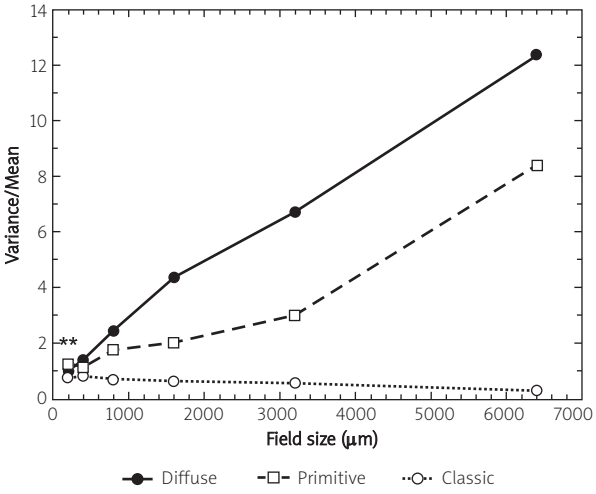

Fig. 1. The spatial patterns of the diffuse, primitive, and classic Aβ deposits in the PHG of a single case (Case C, *PSEN1*).

The frequencies of the different types of spatial pattern (random, regular, regularly distributed clusters, large-scale clustering) were compared between groups using chi-square (χ^2) contingency table tests. In addition, size of the clusters, measured parallel to the pia mater and averaged over all gyri, was compared between groups using two-factor analysis of variance (ANOVA) (STATISTICA software, StatSoft Inc., 2300 East 14th St, Tulsa, OK 74104, USA).

Results

The spatial patterns of the diffuse, primitive, and classic Aβ deposits in the PHG of a single case (Case C, EO-FAD, *PSEN1* mutation) are shown in Fig. 1. The V/M ratio of the diffuse deposits increased with field size without reaching a significant peak consistent with the presence of a large cluster of diffuse Aβ deposits. The V/M ratio of the primitive deposits exhibited a significant peak at a field size of 200 μm, suggesting the presence of clusters of primitive deposits, 200 μm in diameter, regularly distributed parallel to the pia mater. The V/M ratio of the classic deposits was significantly less than unity at all field sizes, suggesting a regular or uniform distribution of deposits.

The frequency of the different types of spatial patterns exhibited by the diffuse, primitive, and classic deposits in EO-FAD, LO-FAD, and SAD is shown in Table II. The diffuse deposits were distributed either in clusters which were regularly distributed parallel to the pia mater or in large clusters, no significant differences in spatial pattern being observed between groups. The primitive Aβ deposits, however, were more frequently distributed in regularly distributed clusters parallel to the pia mater in EO-FAD and LO-FAD and were more frequently distributed in large clusters in SAD ($\chi^2 = 3.94$, $P < 0.05$). In addition, the classic Aβ deposits were less frequently distributed in regular clusters and more frequently distributed in large clusters in EO-FAD compared with LO-FAD ($\chi^2 = 6.45$, $P < 0.05$). The mean cluster sizes of the diffuse, primitive, and

Table II. Frequency of spatial patterns of β-amyloid (Aβ) deposits in early-onset familial Alzheimer's disease (EO-FAD), late-onset familial Alzheimer's disease (LO-FAD), and sporadic Alzheimer's disease (SAD). Data are number of brain regions exhibiting a specific spatial pattern summed over three cortical regions

		Type of spatial pattern			
Group	Aβ	R	Reg	Regular clusters (200-3200 μm)	Large clusters (≥ 3200 μm)
EO-FAD	Diffuse	2	0	6	3
	Primitive	0	0	8	3
	Classic	0	1	5	5
LO-FAD	Diffuse	0	0	8	12
	Primitive	0	0	18	5
	Classic	2	1	11	1
SAD	Diffuse	0	0	22	13
	Primitive	0	0	17	18
	Classic	0	3	13	3

R – random distribution, Reg – regular or uniform distribution
Comparison of frequencies: Chi-square (χ^2) contingency tables: Diffuse deposits, LO-FAD vs. SAD $\chi^2 = 1.83$ ($P > 0.05$), LO-FAD vs. EO-FAD $\chi^2 = 0.86$ ($P > 0.05$), EO-FAD vs. SAD $\chi^2 = 0.03$ ($P > 0.05$); Primitive deposits, LO-FAD vs. SAD $\chi^2 = 3.94$ ($P < 0.05$), LO-FAD vs. EO-FAD $\chi^2 = 0.06$ ($P > 0.05$), EO-FAD vs. SAD $\chi^2 = 1.11$ ($P > 0.05$); Classic deposits, LO-FAD vs. SAD $\chi^2 = 3.74$ ($P > 0.05$), LO-FAD vs. EO-FAD $\chi^2 = 6.45$ ($P < 0.05$), EO-FAD vs. SAD $\chi^2 = 3.14$ ($P > 0.05$)

classic deposits, averaged over cortical regions, are shown in Fig. 2. The mean size of the diffuse deposits differed between groups (F = 3.64, $P < 0.05$), cluster size being significantly less in SAD compared with EO-FAD and LO-FAD. There were no significant differences in the cluster sizes of the primitive (F = 1.89, $P > 0.05$) or classic deposits (F = 0.66, $P > 0.05$) between groups. Within the EO-FAD group, there were no differences in the spatial pattern of the Aβ deposits between APP and PSEN1 cases.

A comparison of the spatial patterns exhibited by the Aβ deposits in cases classified according to *APOE* genotype is shown in Table III. There were no significant differences in the spatial patterns of the diffuse ($\chi^2 = 0.02$, $P < 0.05$), primitive ($\chi^2 = 0.09$, $P < 0.05$), or classic ($\chi^2 = 6.16$, $P < 0.05$) Aβ deposits in cases expressing *APOE* genotypes ε2/3 and ε3/3, compared with those expressing genotypes ε3/4 and ε4/4. The mean cluster sizes of the diffuse, primitive, and classic deposits, averaged over the three cortical regions, are shown in Fig. 3. There were no significant differences in the cluster sizes of the diffuse (F = 0.27, $P > 0.05$) primitive (F = 2.45, $P > 0.05$) or classic deposits (F = 0.61, $P > 0.05$) between cases expressing different *APOE* genotypes, although there is some evidence that the cluster size of the classic deposits may be greater in cases expressing allele ε4.

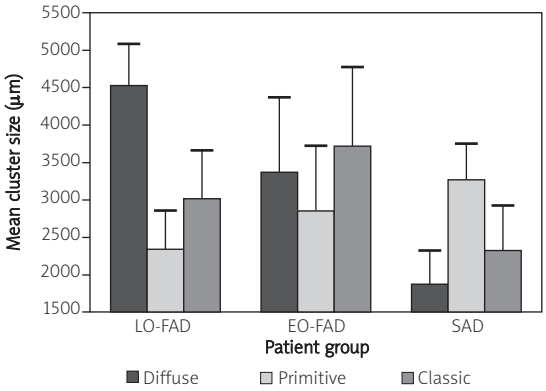

Fig. 2. The mean cluster sizes of the diffuse, primitive, and classic deposits in early-onset familial Alzheimer's disease (EO-FAD), late-onset familial AD (LO-FAD) and sporadic AD (SAD). ANOVA Two-factor: patient group F = 0.11 ($P > 0.05$), Aβ deposit F = 1.92 ($P > 0.05$), Interaction F = 2.00 ($P > 0.05$); one-way for each deposit type: Diffuse F = 3.64 ($P < 0.05$), Primitive F = 1.89 ($P > 0.05$); Classic F = 0.66 ($P > 0.05$).

Table III. Frequency of spatial patterns of Aβ deposits in early-onset familial Alzheimer's disease (EO-FAD), late-onset familial Alzheimer's disease (LO-FAD), and sporadic Alzheimer's disease (SAD) classified according to apolipoprotein (APOE) genotype

		Type of spatial pattern			
APOE genotype	Aβ deposit subtype	R	Reg	Regular clusters (200-3200 μm)	Large clusters (≥ 6400 μm)
ε2/3, ε3/3	Diffuse	0	0	9	6
	Primitive	0	0	10	6
	Classic	0	4	7	2
ε3/4, ε4/4	Diffuse	0	0	12	6
	Primitive	0	0	13	8
	Classic	2	0	7	3

R – random, Reg – regular
Chi-square (χ^2) contingency tables: Diffuse $\chi^2 = 0.02$ ($P > 0.05$), Primitive $\chi^2 = 0.09$ ($P > 0.05$), Classic $\chi^2 = 6.16$ ($P > 0.05$)

Discussion

The Aβ deposits exhibited two common spatial patterns: (1) deposits were clustered with cluster sizes in the size range 200-3200 μm in diameter, the clusters being regularly distributed parallel to the pia mater; and (2) deposits were clustered on a larger scale, usually greater than 3200 μm in diameter, without regular spacing. These results are similar to those previously reported for Aβ deposits [13,15,17] and for NFT [3,11] in AD.

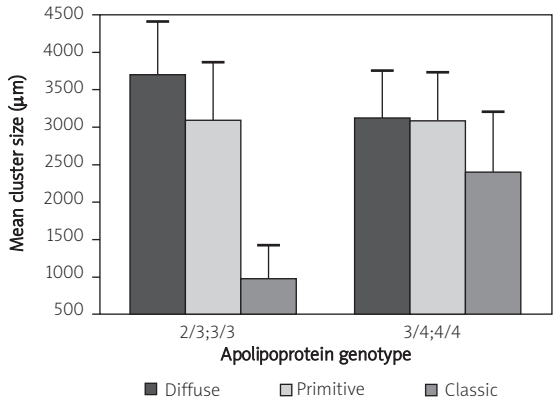

Fig. 3. The mean cluster sizes of the diffuse, primitive, and classic deposits in Alzheimer's disease cases classified according to apolipoprotein (*APOE*) genotype. ANOVA Two-factor: patient group F = 0.27 ($P > 0.05$), Aβ deposit F = 2.45 ($P > 0.05$), Interaction F = 0.61 ($P > 0.05$).

Regular clustering of the diffuse and primitive deposits could be a consequence of degeneration of the cortico-cortical connections [15,24]. In the cerebral cortex, the cells of origin of the cortico-cortical projections are clustered and occur in bands which are regularly distributed along the cortex parallel to the pia mater. Individual bands of cells vary in width approximately from 400 to 1000 μm depending on cortical area [33]. In some gyri, the estimated widths of the clusters of diffuse and primitive Aβ deposits suggest an association with these projections [44]. By contrast, classic deposits often cluster around cerebral blood vessels, especially the vertically penetrating arterioles, which also exhibit a regular pattern of distribution parallel to the pia mater in laminae II/III [9]. By contrast, the large-scale clustering of deposits may be attributable to the aggregation of amyloid within cortical sulci [13]. The density of both neurons and blood vessels is greater in sulci compared with the gyral crest, which could explain these accumulations [4,26].

There were no significant differences in the frequency of the different types of spatial pattern of the diffuse deposits either between EO-FAD, LO-FAD, and SAD, or between cases classified according to *APOE* genotype. Diffuse deposit clusters, however, were larger in EO-FAD and LO-FAD than in SAD, suggesting that initial deposition of Aβ is greater in FAD and that a higher proportion of diffuse deposits may be converted to primitive deposits in SAD [5].

Clusters of primitive deposits were more frequently regularly distributed in EO-FAD and LO-FAD and more frequently present in non-regularly distributed clusters in SAD. Hence, in FAD, conversion of diffuse to primitive deposits may result in a more localized and specific spatial pattern of deposits in relation to the cortico-cortical pathways. By contrast, in SAD, a greater proportion of diffuse deposits may be converted to primitive deposits, resulting in clusters of primitive deposits of similar size to those of FAD and clusters of diffuse deposits smaller than those of FAD.

Classic deposits were less frequently distributed in regular clusters and more frequently present in larger clusters in EO-FAD. Previous studies suggest that classic deposits are more likely to be clustered around blood vessels in SAD than in FAD [12]. Classic deposits also occur with greater density in AD cases with extensive capillary amyloid angiopathy (CAA) [16]. CAA is more frequent in cases with specific gene mutations, APP_{692} mutations, for example, resulting in extensive CAA and numerous large-cored deposits clearly distinct in morphology from those of SAD [21,46]. Hence, in cases with *APP* and *PSEN* mutations, the blood-brain barrier may be significantly damaged, increasing diffusion from blood vessels, and influencing the formation of classic deposits at greater distances from blood vessels than in LO-FAD and SAD.

All types of Aβ deposit exhibited similar spatial patterns and cluster sizes in cases classified according to *APOE* genotype. *APOE* genotype has been identified as a major risk factor in AD, individuals with the disease having 2-3 times the frequency of allele ε4 compared with non-demented elderly controls [51]. The presence of allele ε4 may accelerate the development of AD pathology within the aged brain, and hence is often associated with an earlier disease onset [29]. In addition, the majority of studies report increased amyloid deposition in individuals expressing allele ε4 [18,19,25]. The present data suggest, however, that *APOE* genotype had little effect on the spatial pattern of the Aβ deposits in the frontal and temporal lobe. Some studies suggest that Aβ deposition, specifically in the form of $Aβ_{40}$, may be more closely related to *APOE* genotype [35,39]. Hence, it would be of interest to study the spatial patterns of $Aβ_{40}$ and $Aβ_{42}$ deposits separately in relation to *APOE* genotype.

In conclusion, the data suggest that gene expression had relatively little effect on the type of spatial pattern exhibited by the diffuse Aβ deposits. The average cluster size of the diffuse deposit, however, was larger in FAD compared with SAD, suggesting greater initial Aβ deposition in FAD. However, cluster sizes of the primitive deposits were similar in FAD and SAD, suggesting that (1) a higher proportion of diffuse deposits may be converted to primitive deposits in SAD, and (2) primitive deposits may be more closely related to specific cortico-cortical pathways in FAD. Classic deposits were more extensively distributed in the cortex in FAD than SAD. The presence of the *APOE* allele ε4 had little effect on the spatial patterns or cluster sizes of Aβ deposits.

Acknowledgments

Brain tissue sections were kindly provided by the Brain Bank, Dept. of Neuropathology, Institute of Psychiatry, King's College London, UK. We would like to thank Mrs Mavis Kibble and Mr Alan Brady for technical help with tissue preparation.

References

1. Allsop D, Haga S, Haga C, Ikeda SI, Mann DMA, Ishii T. Early senile plaques in Down's syndrome brains show a close relationship with cell bodies of neurons. Neuropath Appl Neurobiol 1989; 15: 531-542.
2. Armstrong RA. The usefulness of spatial pattern analysis in understanding the pathogenesis of neurodegenerative disorders with particular reference to plaque formation in Alzheimer's disease. Neurodegeneration 1993; 2: 73-80.
3. Armstrong RA. Is the clustering of neurofibrillary tangles in Alzheimer's patients related to the cells of origin of specific cortico-cortical projections? Neurosci Lett 1993; 160: 57-60.
4. Armstrong RA. Quantitative differences in β/A4 protein subtypes in the parahippocampal gyrus and frontal cortex in Alzheimer's disease. Dementia 1994; 5: 1-5.
5. Armstrong RA. β-amyloid plaques: stages in life history or independent origin? Dement Geriatr Cogn Disord 1998; 9: 227-238.
6. Armstrong RA. Diffuse β-amyloid (Aβ) deposits and neurons: in situ secretion or diffusion of Aβ? Alz Rep 2001; 3: 289-294.
7. Armstrong RA. Quantifying the pathology of neurodegenerative disorders: quantitative measurements, sampling strategies and data analysis. Histopathology 2003; 42: 521-529.
8. Armstrong RA. Plaques and tangles and the pathogenesis of Alzheimer's disease. Folia Neuropathol 2006; 44: 1-11.
9. Armstrong RA. Classic β-amyloid deposits cluster around large diameter blood vessels rather than capillaries in sporadic Alzheimer's disease. Curr Neurovasc Res 2006; 3: 289-294.
10. Armstrong RA. Measuring the spatial arrangement patterns of pathological lesions in histological sections of brain tissue. Folia Neuropathol 2007; 44: 229-237.

11. Armstrong RA. Clustering and periodicity of neurofibrillary tangles in the upper and lower cortical laminae in Alzheimer's disease. Folia Neuropathol 2008; 46: 26-31.
12. Armstrong RA. Spatial correlations between β-amyloid (Aβ) deposits and blood vessels in familial Alzheimer's disease. Folia Neuropathol 2009; 46: 241-248.
13. Armstrong RA. A spatial pattern analysis of β-amyloid (Aβ) deposition in the temporal lobe in Alzheimer's disease. Folia Neuropathol 2010; 48: 67-74.
14. Armstrong RA. Quantitative methods in neuropathology. Folia Neuropathol 2010; 48: 217-230.
15. Armstrong RA, Myers D, Smith CUM. The spatial patterns of β/A4 deposits in Alzheimer's disease. Acta Neuropathol 1993; 86: 36-41.
16. Armstrong RA, Myers D, Smith CUM. The ratio of diffuse to mature beta/A4 deposits in Alzheimer's disease varies in cases with and without pronounced congophilic angiopathy. Dementia 1993; 4: 251-255.
17. Armstrong RA, Cairns NJ. Analysis of β-amyloid (Aβ) deposition in the temporal lobe in Alzheimer's disease using Fourier (spectral) analysis. Neuropathol Appl Neurobiol 2010; 36: 248-257.
18. Beffert U, Poirier J. Apolipoprotein E, plaques, tangles and cholinergic dysfunction in Alzheimer's disease. Anns NY Acad Sci 1996; 777: 166-174.
19. Berr C, Hauw JJ, Delaere P, Duyckaerts C, Amouyel P. Apolipoprotein E allele e4 is linked to increased deposition of the amyloid β-peptide (Aβ) in cases with or without Alzheimer's disease. Neurosci Lett 1994; 178: 221-224.
20. Chartier-Harlin MC, Crawford F, Houlden H, Warren A, Hughes D, Fidani L, Goate A, Rossor M, Rocques P, Hardy J, Mullan M. Early onset Alzheimer's disease caused by mutations at codon 717 of the β-amyloid precursor protein gene. Nature 1991; 353: 844-846.
21. Cras P, van Harskamp F, Hendricks L, Centerick C, van Duyn CM, Stefanko SZ, Hofman A, Kris JM, van Broekhoven C, Martin JJ. Presenile Alzheimer's dementia characterized by amyloid angiopathy and large amyloid type senile plaques in the APP692 Ala->Gly mutation. Acta Neuropathol 1998; 96: 253-260.
22. Delaere P, Duyckaerts C, He Y, Piette F, Hauw JJ. Subtypes and differential laminar distribution of β/A4 deposits in Alzheimer's disease: relationship with the intellectual status of 26 cases. Acta Neuropathol 1991; 81: 328-335.
23. Delacourte A, Sergeant N, Champain D. Wattez A, Maurage CA, Lebert F, Pasquier F, David JP. Nonoverlapping but synergetic tau and amyloid precursor protein pathologies in sporadic Alzheimer's disease. Neurology 2002; 59: 398-407.
24. De Lacoste M, White CL. The role of cortical connectivity in Alzheimer's disease pathogenesis: a review and model system. Neurobiol Aging 1993; 14: 1-16.
25. Gearing M, Schneider JA, Robins RS, Hollister RD, Mori H, Games D, Hyman BT, Mirra SS. Regional variations in the distribution of Apolipoprotein E and Aβ in Alzheimer's disease. J Neuropath Exp Neurol 1995; 54: 833-841.
26. Gentleman SM, Williams B, Roystan MC, Jagoe R, Clinton J, Perry RH, Ince PG, Allsop D, Polak JM, Roberts GW. Quantification of β/A4 protein deposition in the medial temporal lobe: A comparison of Alzheimer's disease and senile dementia of the Lewy Body Type. Neurosci Lett 1992; 142: 9-12.
27. Glenner GG, Wong CW. Alzheimer's disease and Down's syndrome: sharing of a unique cerebrovascular amyloid fibril protein, Biochem Biophys Res Commun 1984; 122: 1131-1135.
28. Goate R, Chartier-Harlin M-C, Mullan M, Brown J, Crawford F, Fidani L, Giuffra L, Haynes A, Irving N, James L, Mant R, Newton P, Rooke K, Roques P, Talbot C, Pericak-Vance, Roses A, Williamson R, Rossor M, Owen M, Hardy J. Segregation of a missense mutation in the amyloid precursor protein gene with familial Alzheimer's disease. Nature (London) 1991; 349: 704-706.
29. Gomez-Isla T, West HL, Rebeck GW, Harr SD, Growdon JH, Lacascio JJ, Perls TT, Lipsitz LA, Hyman BT. Clinical and pathological correlates of apolipoprotein E e4 in Alzheimer's disease. Ann Neurol 1996; 39: 62-70.
30. Grazini M, Prabas J, Silva F, Oliveira S, Santana I, Oliveira C. Genetic basis of Alzheimer's dementia: role of mitochondrial DNA mutations. Genes, Brain, and Behaviour 2006; 5 (supp 2): 92-107.
31. Greenberg BD. The COOH-terminus of the Alzheimer amyloid Aß peptide: Differences in length influence the process of amyloid deposition in Alzheimer brain, and tell us something about relationships among parenchymal and vessel-associated amyloid deposits. Amyloid: Int J Exp Clin Invest 1995; 2: 195-203.
32. Hardy JA, Higgins GA. Alzheimer's disease: The amyloid cascade hypothesis. Science 1992; 256: 184-185.
33. Hiorns RW, Neal JW, Pearson RCA, Powell TPS. Clustering of ipsilateral cortico-cortical projection neurons to area 7 in the rhesus monkey. Proc R Soc London 1991; 246: 1-9.
34. Hoenicka J. Genes in Alzheimer's disease. Revista de Neurolgia 2006; 42: 302-305.
35. Ishii K, Lippa C, Tomiyama T, Miyatake F, Ozawa K, Tamaoka A, Hasegawa T, Fraser P, Shoji S, Nee L, Pollen D, St George-Hyslop P, Ii K, Ohtake T, Kalaria R, Rossor M, Lantos P, Cairns N, Farrer L, Mori H. Distinguishable effects of Presenilin-1 and APP717 mutations on amyloid plaque deposition. Neurobiol Aging 2001; 22: 367-376.
36. Jellinger KA, Bancher C. Neuropathology of Alzheimer's disease: a critical update. J Neural Transm 1998; 54: 77-95.
37. Kayed R, Head E, Thompson JL, McIntire TM, Milton SC, Cotman CW, Glabe CG. Common structure of soluble amyloid oligomers implies common mechanism of pathogenesis. Science 2003; 300: 486-489.
37. Levy-Lahad E, Wijsman EM, Nemens E, Anderson L, Goddard KAB, Weber JL, Bird TD, Schellenberg GD. A familial Alzheimer's disease locus on chromosome 1. Science 1995; 269: 970-973.
38. Mann DMA, Iwatsubo T, Pickering-Brown SM, Owen F, Saido TC, Perry RH. Preferential deposition of amyloid beta protein (A beta) in the form of A beta (40) in Alzheimer's disease is associated with a gene dosage effect of the apolipoprotein E E4 allele. Neurosci Lett 1997; 221: 81-84.
39. McCauley JL, Hahs DW, Jiang L, Scott WK, Welsh-Bohmer KA, Jackson CE, Vance JM, Pericak-Vance MA, Haines JL. Combina-

torial Mismatch Scan (CMS) for loci associated with dementia in the Amish BMC. Medical Genetics 2006; 7: 19.
40. Miller DL, Papayannopoulos IA, Styles J, Bobin SA, Lin YY, Biemann K, Iqbal K. Peptide compositions of the cerebrovascular and senile plaque core amyloid deposits of Alzheimer's disease. Arch Biochem Biophys 1993; 301: 41-52.
41. Mirra SS, Heyman A, McKeel D, Sumi SM, Crain BJ, Brownlee LM, Vogel FS, Hughes JP, van Belle G, Berg L et al. The consortium to establish a registry for Alzheimer's disease (CERAD). II. Standardization of the neuropathological assessment of Alzheimer's disease. Neurology 1991; 41: 479-486.
42. Newell KL, Hyman BT, Growden JH, Hedley-Whyte ET. Application of the National Institute on Aging (NIA)-Reagan Insitute criteria for the neuropathological diagnosis of Alzheimer's disease. J Neuropathol Exp Neurol 1999; 58: 1147-1155.
43. Pearson RCA, Esiri MM, Hiorns RW, Wilcock GK, Powell TPS. Anatomical correlates of the distribution of the pathological changes in the neocortex in Alzheimer's disease. Proc Natl Acad Sci USA 1985; 82: 4531-4534.
44. Roher AE, Lowenson JD, Clarke S, Wolkow C, Wang R, Cotter RJ, Reardon IM, Zurcherneely HA, Henrikson RL, Ball MJ, Greenberg BD. Structural alterations in the peptide backbone of β-amyloid core protein may account for its deposition and stability in Alzheimer's disease. J Biol Chem 1993; 268: 3072-3073.
45. Roks G, Van Harskamp F, De Koning I, Cruts M, de Jonghe C, Kumar-Singh S, Tibben A, Tanghe H, Niermeijer MF, Hofman A, Van Swieten JC, Van Broeckhoven C, Van Duijn CM. Presentation of amyloidosis in carriers of the codon 692 mutation in the amyloid precursor protein gene (APP692). Brain 2000; 123: 2130-2140.
46. Saunders A, Strittmatter W, Schmechel D, St. George-Hyslop P, Pericak-Vance M, Joo S, Rose B, Gasella J, Crapper-MacLachan D, Albersts M, Hulette C, Crain B, Goldgaber D, Roses A. Association of apolipoprotein E allele e4 with late-onset familial and sporadic Alzheimer's disease. Neurology 1993; 43: 1467-1472.
47. Sherrington R, Rogaev E, Liang Y, Rogaeva E, Levesque G, Ikeda M, Chi H, Lin C, Li G, Holman K, Tsuda T, Mar L, Foncin J, Bruni A, Moulese M, Sorbi S, Rainero I, Pinessi L, Nee L, Chumakov I, Pollen D, Brookes A, Sauseau P, Polinski R, Wasco R, Dasilva H, Haines J, Pericak-Vance M, Tanzi R, Roses A, Fraser P, Rommens J, St George-Hyslop P. Cloning of a gene bearing missense mutations in early onset familial Alzheimer's disease. Nature 1993; 375: 754-760.
48. Sillen A, Forsell C, Lilius L, Axwlman K, Bjork B, Onkamo P, Kere J, Winblad B, Graff C. Genome scan on Swedish Alzheimer disease families. Mole Psy 2006; 11: 182-186.
49. Spargo E, Luthert PJ, Anderton BH, Bruce M, Smith D, Lantos PL. Antibodies raised against different proteins of A4 protein identify a subset of plaques in Down's syndrome. Neurosci Lett 1990; 115: 345-350.
50. Strittmatter WJ, Weisgraber KH, Huang DY, Dong LM, Salvasan GS, Pericak-Vance M, Schmechel D, Saunders AM, Goldgaber D, Roses AD. Binding of human apoliprotein E to synthetic amyloid-β-peptide: isoform-specific effects and implications for late-onset Alzheimer's disease. Proc Natl Acad Sci USA 1993; 90: 8098-8102.
51. Tierney MC, Fisher RH, Lewis AJ, Zorzitto ML, Snow WG, Reid DW, Nieuwstraten P. The NINCDS-ADRDA work group criteria for the clinical diagnosis of probable Alzheimer's disease. Neurology 1988; 38: 359-364.